Physics of the Earth and Planetary Interiors 274 (2018) 14–22

Contents lists available at ScienceDirect

Physics of the Earth and Planetary Interiors

journal homepage: www.elsevier.com/locate/pepi

The Burgers/squirt-flow seismic model of the crust and mantle

José M. Carcione*, Flavio Poletto, Biancamaria Farina

Istituto Nazionale di Oceanografia e di Geofisica Sperimentale (OGS), Borgo Grotta Gigante 42c, 34010 Sgonico, Trieste, Italy

ARTICLE INFO

Keywords:
Seismic waves
Burgers model
Squirt-flow model
Partial melting
Attenuation

ABSTRACT

Part of the crust shows generally brittle behaviour while areas of high temperature and/or high pore pressure, including the mantle, may present ductile behaviour. For instance, the potential heat source of geothermal fields, overpressured formations and molten rocks. Seismic waves can be used to detect these conditions on the basis of reflection and transmission events. Basically, from the elastic-plastic point of view the seismic properties (seismic velocity, quality factor and density) depend on effective pressure and temperature. Confining and pore pressures have opposite effects on these properties, and high temperatures may induce a similar behaviour by partial melting. In order to model these effects, we consider a poro-viscoelastic model based on the Burgers mechanical element and the squirt-flow model to represent the properties of the rock frame to describe ductility in which deformation takes place by shear plastic flow, and to model local and global fluid flow effects.

The Burgers element allows us to model the effects of the steady-state creep flow on the dry-rock frame. The stiffness components of the brittle and ductile media depend on stress and temperature through the shear viscosity, which is obtained by the Arrhenius equation and the octahedral stress criterion. Effective pressure effects are taken into account in the dry-rock moduli by using exponential functions whose parameters are obtained by fitting experimental data as a function of confining pressure. Since fluid effects are important, the density and bulk modulus of the saturating fluids (water at sub- and supercritical conditions) are modeled by using the equations provided by the NIST website. The squirt-flow model has a single free parameter represented by the aspect ratio of the grain contacts. The theory generalizes a preceding theory based on Gassmann (low-frequency) moduli to the more general case of the presence of local (squirt) flow and global (Biot) flow, which contribute with additional attenuation mechanisms to the wave propagation.

1. Introduction

The upper crust shows generally brittle behaviour while deeper zones, including the mantle, may present ductile behaviour with partial melt, depending on the pressure-temperature conditions (e.g., Meissner and Strehlau, 1982; Williams and Garnero, 1996; Tauzin et al., 2010). Seismic waves can be used to detect these conditions on the basis of wave velocity and attenuation. Early models explain the seismic low-velocity zones (e.g., asthenosphere) as a region of partially molten rock (Walsh, 1969). Mavko and Nur (1975) suggest that a reasonable mechanism for transient deformation in the upper mantle is small-scale flow of partial melt. Schmeling (1985) discusses and reviews such models. However, Karato and Jung (1998) claim that melt alone cannot explain the observations and suggest a model by which water enhances anelastic relaxation and partial melting causes water removal from minerals. If melted material completely wets grain-boundaries, a small amount of melt is enough to reduce the seismic wave velocities (Karato, 2014). Therefore, a combined effect of melt and water relaxation seems to explain seismic velocity in the crust and mantle. Karato and Jung (1998) report a quality factor $Q \propto \omega^{-\gamma}$, where ω is the angular frequency and $\gamma = 0.1$–0.3. Their model includes a temperature dependence of Q through an Arrhenius type equation. Takei (2002) investigated the effect of pore geometry based on Gassmann equations and various theories including several aspect-ratio models.

We consider a constitutive equation including ductility (and melt), through the Burgers mechanical model, and anelastic (seismic) relaxation described by the squirt-flow model, based on Biot's theory. We model the shear stiffness modulus using the Burgers model, where ductility depends on temperature, depth and in situ pressures. The rock (Burgers) viscosity is obtained by the Arrhenius equation and the octahedral stress criterion (Carcione and Poletto, 2013; Carcione et al., 2014). The only attenuation mechanism obtained from the dispersion equation of Biot's theory is the so-called global flow, that is, wavelength-scale equilibration between the peaks and troughs of the wave (Biot, 1962; Carcione, 2014). This mechanism is due to the viscous nature of the pore-fluid, as well as the mesoscopic loss, where the

* Corresponding author.
E-mail address: jcarcione@inogs.it (J.M. Carcione).

https://doi.org/10.1016/j.pepi.2017.10.008
Received 22 June 2017; Received in revised form 18 October 2017; Accepted 23 October 2017
Available online 28 October 2017
0031-9201/

mesoscopic-scale length is much larger than the grain sizes but much smaller than the wavelength of the pulse. In this case the rock permeability plays tan important role. Experimental evidence can be found in Batzle et al. (2006), and a theoretical analysis can be found several works, notably Pride et al. (2004) and Carcione and Picotti (2006).

Another important loss mechanism is the so-called "squirt flow", by which there is flow from fluid-filled microcracks (grain contacts) to the pore space and vice versa (Mavko et al., 2009; Carcione, 2014). Biot (1962) was the first to discuss this mechanism and proposed a viscoelastic mechanical model to describe it. The problem resides in finding a suitable squirt-flow model, in which the parameters can be entirely estimated from the microstructural properties of the rock. Such a model has recently been proposed by Gurevich et al. (2010) (see Carcione and Gurevich, 2011). The density and bulk modulus of the saturating fluids (water and steam) are modeled by using the equations provided by the National Institute of Standards and Technology (NIST) website, including supercritical behaviour. The new model describes seismic attenuation by the combined effect of rock ductility (partially melting) and squirt flow.

Crustal values of Q have been determined by Castro et al. (2008), that can be useful to calibrate the model. Apart from intrinsic dissipation, in inhomogeneous media waves can experience the so called apparent attenuation due to scattering. Hoshiba (1993) measured intrinsic absorption and scattering attenuation from earthquake sources using the multiple lapse time window analysis. Rachman and Chung (2016) used the same technique to measure attenuation down to the brittle-ductile transition. Here, shear seismic attenuation include both intrinsic absorption and scattering losses described by a Zener kernel.

2. Theory

2.1. The Burgers model for brittle-ductile behaviour

The constitutive equation, including both the shear viscoelastic and ductile behaviour, can be described with the Burgers model as reported in Carcione and Poletto (2013) and Carcione et al. (2014). The Burgers model is a series connection of a dashpot and a Zener model (Fig. 1)a and its complex shear modulus can be written as

$$\mu_B = \frac{\mu_0(1 + i\omega\tau_\epsilon)}{1 + i\omega\tau_\sigma - \frac{i\mu_0}{\omega\eta}(1 + i\omega\tau_\epsilon)}. \tag{1}$$

The quantities τ_σ and τ_ϵ are seismic relaxation times, μ_0 is the relaxed shear modulus (see below) and η is the flow viscosity describing the ductile behaviour. The relaxation times can be expressed as

$$\tau_\epsilon = \frac{\tau_0}{Q_0}\left(\sqrt{Q_0^2 + 1} + 1\right), \quad \tau_\sigma = \tau_\epsilon - \frac{2\tau_0}{Q_0}, \tag{2}$$

where τ_0 is a relaxation time such that $\omega_0 = 1/\tau_0$ is the center frequency of the relaxation peak and Q_0 is the minimum quality factor.

The limit $\eta \to \infty$ in Eq. (1) recovers the Zener kernel to describe the behaviour of the brittle material, while $\tau_\sigma \to 0$ and $\tau_\epsilon \to 0$ yield the Maxwell model used by Dragoni and Pondrelli (1991): $\mu_B = \mu_0(1 - i\mu_0/\omega\eta)^{-1}$ (e.g., Carcione, 2014). For $\eta \to 0, \mu_B \to 0$ and the medium becomes a fluid. Moreover, if $\omega \to \infty, \mu_B \to \mu_0\tau_\epsilon/\tau_\sigma$, where μ_0 is the relaxed ($\omega = 0$) shear modulus of the Zener element ($\eta = \infty$).

The viscosity η can be expressed by the Arrhenius equation (e.g., Carcione et al., 2006; Montesi, 2007). It is related to the steady-state creep rate $\dot{\epsilon}$ by

$$\eta = \frac{\sigma_o}{2\dot{\epsilon}}, \quad \dot{\epsilon} = A\sigma_o^n \exp(-E/RT) \tag{3}$$

where σ_o is the octahedral stress (e.g., Gangi, 1981; Carcione et al., 2006; Carcione and Poletto, 2013), A and n are constants, E is the activation energy, $R = 8.3144$ J/mol/°K is the gas constant and T is the absolute temperature. The parameters of the empirical relation (3) are determined by performing laboratory experiments at different strain rates, temperatures and/or stresses (e.g. Gangi, 1983; Ranalli, 1997; Fogler, 2005; Avramov, 2007)

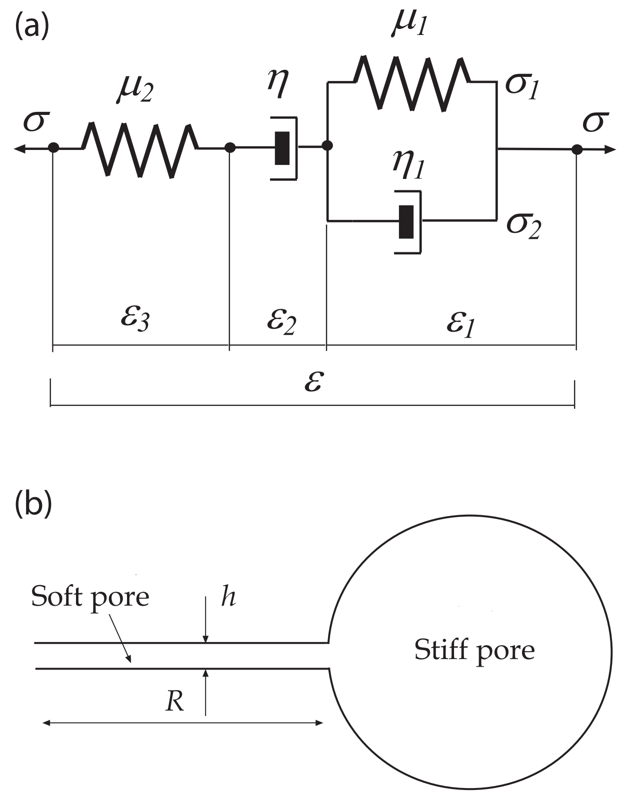

Fig. 1. Mechanical representation of the Burgers viscoelastic model for shear deformations (a) (e.g., Carcione, 2014). σ, ϵ, μ and η represent stress, strain, shear modulus and viscosity, respectively, where η_1 describes seismic relaxation while η is related to plastic flow and processes such as dislocation creep. Sketch of the squirt-flow model (b), where two sandstone grains in contact are shown. The soft pores are the grain contacts and the stiff pores constitute the main porosity. The quantity R is the radius of the disk-shaped soft pore (half disk is represented in the plot).

The octahedral stress is

$$\sigma_o = \frac{1}{3}\sqrt{(\sigma_v - \sigma_h)^2 + (\sigma_v - \sigma_H)^2 + (\sigma_h - \sigma_H)^2}, \tag{4}$$

where the σ's are the stress components in the principal system, corresponding to the vertical (v) lithostatic stress, and the maximum (H) and minimum (h) horizontal tectonic stresses.

The temperature is a function of depth through the geothermal gradient G. A linear approximation is $T = zG$, where z is the depth.

2.2. The squirt-flow model

In the absence of external sources, the time-differentiated stress-strain relations for an inhomogeneous isotropic poroelastic medium, according to Biot's theory are

$$\dot{\sigma}_{ij} = 2\mu_G * d_{ij} + K_G\vartheta\delta_{ij} + \alpha M\varphi\delta_{ij},$$
$$\dot{p}_f = -M(\varphi + \alpha\vartheta),$$
$$\text{where } \vartheta \equiv \nabla\cdot\mathbf{v},\ \varphi \equiv \nabla\cdot\mathbf{q},\ d_{ij} \equiv \tfrac{1}{2}(\partial_i v_j + \partial_j v_i) - \tfrac{1}{3}\delta_{ij}\vartheta, \tag{5}$$

(Biot, 1962; Carcione, 2014), where σ_{ij} are the total stress components, p_f is the phase-averaged pressure fluctuation in the fluid, $\mathbf{v}$ is the phase-averaged particle-velocity vector of the solid constituent of the two-phase poroelastic medium, with components v_i, and $\mathbf{q}$ is the porosity-weighted relative fluid velocity with respect to the solid. The quantities μ_G, K_G, M and α are poroelasticity coefficients defined below. A dot above a variable denotes time differentiation, ∂_i denotes spatial differentiation with respect to the x_i-coordinate, δ_{ij} is the Kronecker delta and

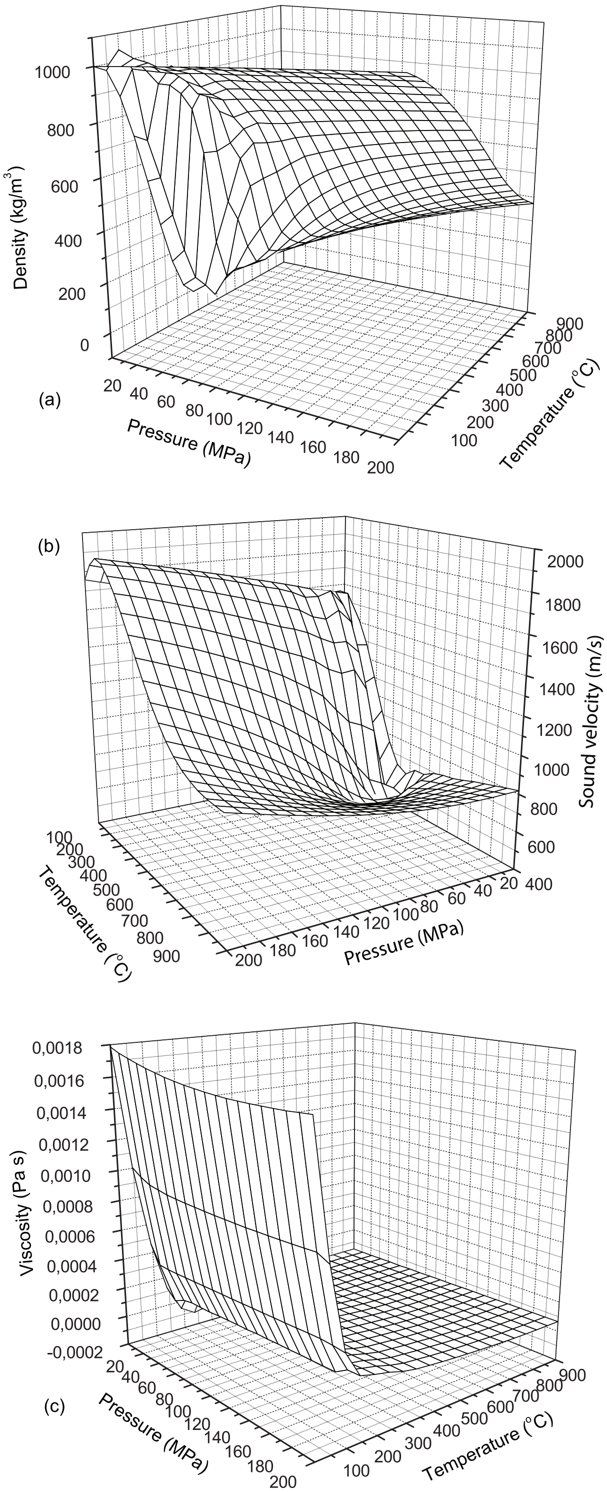

Fig. 2. Water density (a), sound velocity (b) and viscosity (c) for a wide range of pressures and temperatures (data taken from the NIST website).

the symbol "$*$" denotes time convolution. The stress-strain relations are written in the particle-velocity/stress formulation, which is suitable to perform numerical simulations. The time convolution arises from the fact that μ_B in Eq. (1) depends on frequency and for simplicity its time-domain dependence (a relaxation function) is denoted with the same symbol.

The poroelasticity coefficients in Eq. (5) are the Gassmann bulk and shear moduli,

$$K_G = K_m + \alpha(K_m)^2 M(K_m) \quad \text{and } \mu_G = \mu_m = \mu_B \tag{6}$$

and

$$\alpha(K_m) = 1 - \frac{K_m}{K_s} \quad \text{and } M(K_m) = \frac{K_s}{1-\phi-K_m/K_s + \phi K_s/K_f}, \tag{7}$$

where ϕ is the porosity, K_m and μ_m are the bulk and shear moduli of the drained matrix, and K_s and K_f are the solid and fluid bulk moduli, respectively (e.g., Carcione, 2014; Carcione et al., 2017). We explicitly indicate the functional form of α and M on K_m, since we shall replace this modulus by a modified matrix (or frame) complex modulus K, which includes the squirt-flow mechanism. In the same manner, μ_m will be replaced by μ. The new moduli are complex-valued and frequency-dependent.

The squirt flow model is based on the fact that the pore space of many rocks has a binary structure: relatively stiff pores, which constitute the majority of the pore space, and relatively compliant (or soft) pores, which are responsible for the pressure dependency of the poroelastic moduli. When the frequency is higher than the squirt characteristic frequency, the fluid pressure doesn't have enough time to equilibrate between stiff and compliant pores during a half wave cycle (the so called unrelaxed state). Then, compliant pores at the grain contacts are effectively isolated from the stiff pores and hence become stiffer with respect to normal (but not tangential) deformation. In order to model the frequency dependency of the moduli, Gurevich et al. (2010) assumed a geometrical configuration by which a compliant pore forms a disk-shaped gap between two grains, and its edge opens into a toroidal stiff pore (Fig. 1b).

Using this model, the bulk and shear moduli of the saturated rock at low frequencies are given by Gassmann's equations,

$$K_G = K + \alpha^2(K)M(K) \quad \text{and } \mu_G = \mu, \tag{8}$$

where K and μ are the bulk and shear moduli of the modified frame including the un-relaxation due to the presence of the squirt-flow mechanism, and α and M are given by Eq. (7) substituting K_m with K. For simplicity, we keep the same notation for the Gassmann moduli, but now they are complex-valued and frequency-dependent.

Gurevich et al. (2010) obtained the modified dry moduli in the following form

$$\begin{aligned} \frac{1}{K} &= \frac{1}{K_h} + \left[\left(\frac{1}{K_m} - \frac{1}{K_h}\right)^{-1} + \left(\frac{1}{K_f^*} - \frac{1}{K_s}\right)^{-1} \phi_c^{-1}\right]^{-1}, \\ \frac{1}{\mu} &= \frac{1}{\mu_m} - \frac{4}{15}\left(\frac{1}{K_m} - \frac{1}{K}\right), \end{aligned} \tag{9}$$

where K_m and μ_m are the dry-rock bulk and shear moduli at the confining pressure p_c,K_h is the dry-rock bulk modulus at a confining pressure where all the compliant pores are closed, i.e., an hypothetical rock without the soft porosity, and ϕ_c is the compliant porosity. This is so small – nearly 0.001 for most rocks – that the total porosity ϕ can be assumed to be equal to the stiff porosity. The key quantity in Eqs. (9) is the effective bulk modulus of the fluid saturating the soft pores:

$$K_f^* = \left[1 - \frac{2J_1(kR)}{kRJ_0(kR)}\right]K_f, \quad k = \frac{2}{h}\sqrt{-\frac{3i\omega\eta_f}{K_f}}, \tag{10}$$

where J_0 and J_1 are Bessel functions, η_f is the fluid shear viscosity, R is the radius of the crack and h is its thickness (see Fig. 1b). If the fluid modulus satisfies

$$K_f \gg 8\phi_c\left(\frac{1}{K_m} - \frac{1}{K_h}\right)^{-1}, \tag{11}$$

we have the approximation

$$K_f^* = i\omega\eta^*, \tag{12}$$

where

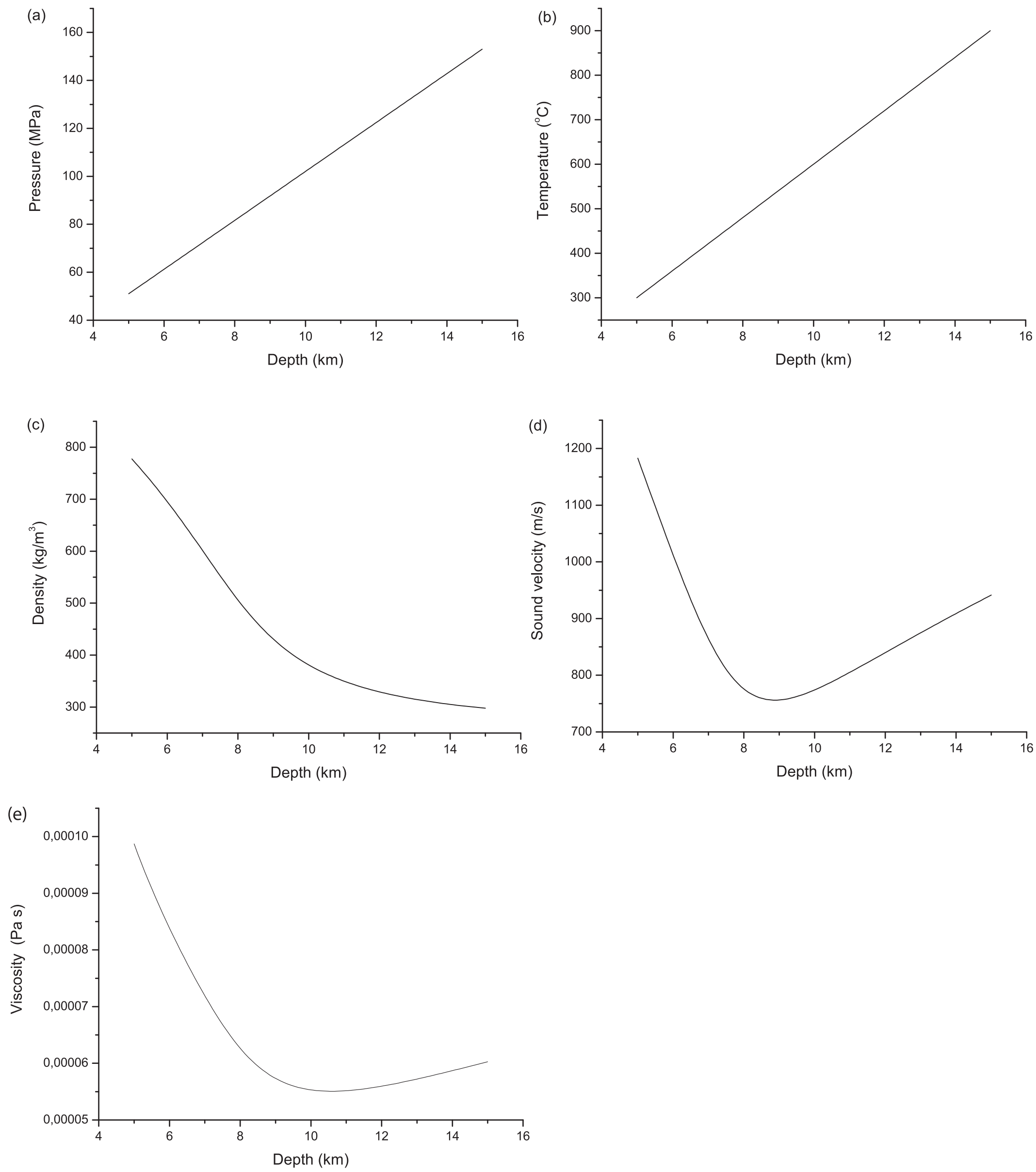

Fig. 3. Pore pressure (a), temperature (b), water density (c) water sound velocity (d) and water viscosity (e) as a function of depth, according to the NIST website.

$$\eta^* = \frac{3}{2}\left(\frac{R}{h}\right)^2 \eta_f, \tag{13}$$

is an effective viscosity.

The peak relaxation frequency of the squirt-flow model is (Carcione and Gurevich, 2011)

$$f_{sf} \approx \frac{K_s}{3\pi\eta_f a}\left(\frac{h}{R}\right)^2, \quad a = (K_s/\phi_c)(1/K_m - 1/K_h), \tag{14}$$

using the approximations $K_h \approx K_m$ and $a \gg 1$. Hence, the peak frequency decreases with increasing viscosity and decreasing aspect ratio of the crack.

The squirt-flow model is consistent with Gassmann's theory in the low-frequency limit, and with Mavko-Jizba unrelaxed moduli in the high-frequency limit (Mavko and Jizba, 1991). All the parameters of the model have a clear physical meaning. There is only one adjustable parameter: the aspect ratio of compliant pores (grain contacts) h/R.

In order to include the pressure dependence, we express the dry-rock bulk moduli as

$$K_m = K_0 g_1(p_d), \quad \text{and } \mu_m = \mu_B g_2(p_d), \tag{15}$$

where $g_r(p_d)$, $r = 1,2$ defines the dependence of the moduli on the differential pressure $p_d = p_c - p$, where p_c is the confining pressure, p is the average pore pressure and K_0 is the bulk modulus at infinite effective pressure. Moreover, if $\eta = \infty, \omega = 0$ and $p_d = \infty$ we obtain $\mu_m = \mu_0$. The simplest form of function g, in good agreement with experimental data, is

$$g_r(p_d) = 1 - (1 - a_r)\exp(-p_d/p_r^*), \quad r = 1,2 \tag{16}$$

(Kaselow and Shapiro, 2004), where a_r and p_r^* are parameters. It is $g_r = 1$ for $p_d \to \infty$ (e.g., very high confining pressure) and $g_r = a_r$ for $p_d \to 0$ (pore pressure equal to the confining pressure).

The bulk density is

$$\rho = (1 - \phi)\rho_s + \phi\rho_f, \tag{17}$$

where ρ_s and ρ_f are the grain and fluid densities, respectively.

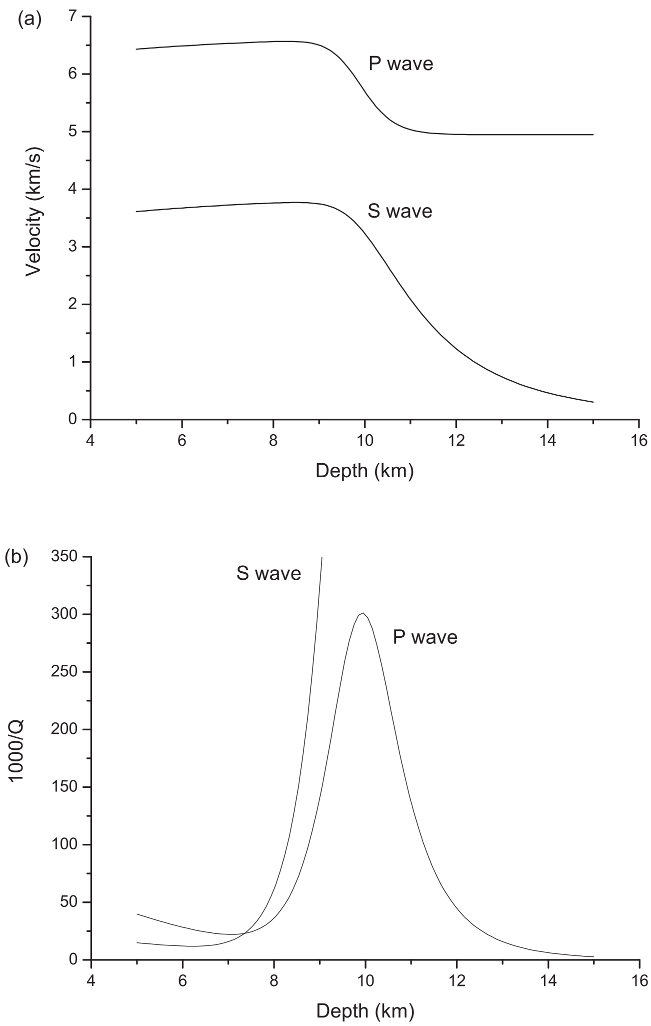

Fig. 4. Seismic velocities (a) and quality factors (b) as a function of depth. The frequency is 10 Hz.

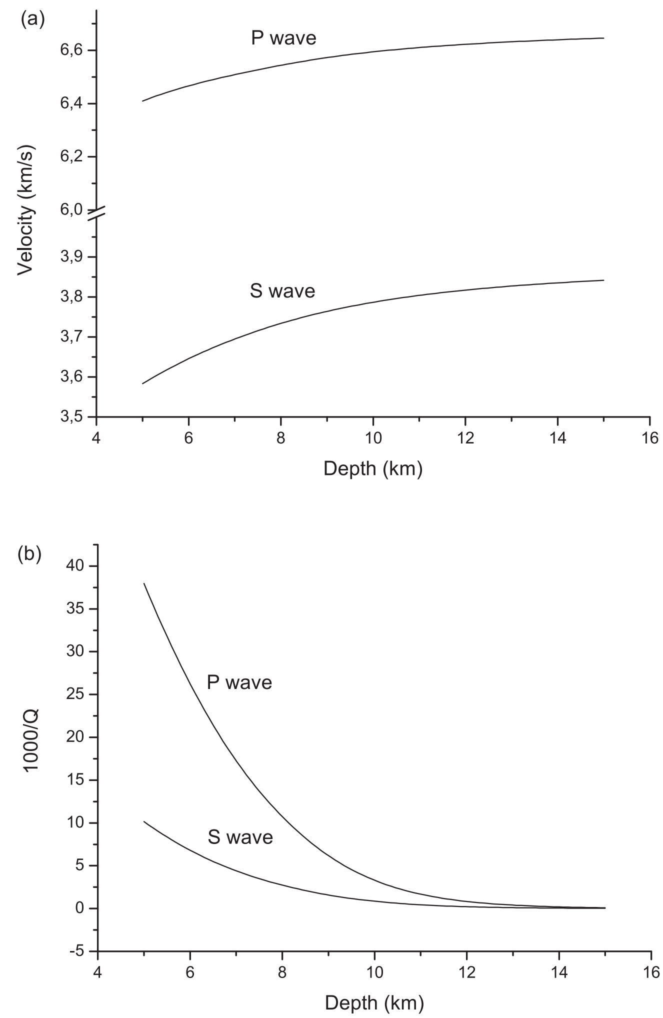

Fig. 5. Seismic velocities (a) and quality factors (b) as a function of depth, without the Burgers mechanism. The frequency is 10 Hz.

3. Phase velocity and dissipation factor

The phase velocity and dissipation factor (inverse of the quality factor), including the Burgers, Biot and squirt-flow losses, are

$$v_p = \left[\mathrm{Re}\left(\frac{1}{v_c}\right)\right]^{-1}, \tag{18}$$

and

$$Q^{-1} = \frac{\mathrm{Im}(v_c^2)}{\mathrm{Re}(v_c^2)} \tag{19}$$

where v_c is the complex velocity (e.g., Carcione, 2014). For shear waves

$$v_c = \sqrt{\frac{\mu}{\bar{\rho}}}, \quad \bar{\rho} = \rho - \rho_f^2/\rho_1 \tag{20}$$

where

$$\rho_1 = \frac{\rho_f \mathscr{T}}{\phi} + \frac{\eta_f}{\mathrm{i}\omega\kappa}, \tag{21}$$

where $\mathscr{T}$ is the rock tortuosity and κ is the permeability. Here we assume $\mathscr{T} = 1-0.5(1-1/\phi)$ (Mavko et al., 2009).

The complex velocity of the P waves is obtained from the following second-order equation:

$$\bar{\rho}\rho_1 v_c^4 + a_1 v_c^2 + a_0 = 0, \tag{22}$$

where

$$a_1 = (2\alpha\rho_f - \rho)M - \rho_1\left(K_G + \tfrac{4}{3}\mu_G\right),$$
$$a_0 = \left(K + \tfrac{4}{3}\mu\right)M \tag{23}$$

(e.g., Carcione, 2014 eq. (7.324)).

Manning and Ingebritsen (1999) inferred permeability from thermal modeling and metamorphic systems suggesting the following dependence with depth z,

$$\log\kappa = -3.2\,\log z - 14 = -3.2\,\log\left(\frac{T}{G}\right) - 14. \tag{24}$$

where z is the depth in km and the permeability is given in m^2. The second expression assumes a linear geothermal law, $T = zG$.

4. Example

We consider sample KTB 61C9b (amphibolite) reported in Popp and Kern (1994) (their Table II and Fig. 3). The "crack-free" dry- and wet-rock S-wave velocities are 3880 m/s and 3820 m/s, respectively, where "crack-free" means that the compliant pores are closed. We assume $\rho_s = 3000\ \mathrm{kg/m^3}$ and consider the water properties at 20 °C and 80 MPa, such that $\rho_f = 1033\ \mathrm{kg/m^3}$ and $K_f = 2.7$ GPa. From Gassmann equation, stating that the dry-rock and the wet-rock shear moduli are equal, we have that $\mu_h = \rho_s(1-\phi)3880^2 = [\phi\rho_f + (1-\phi)\rho_s]3820^2 = 41.5$ GPa, and therefore $\phi = 8.4\%$. The mineral bulk

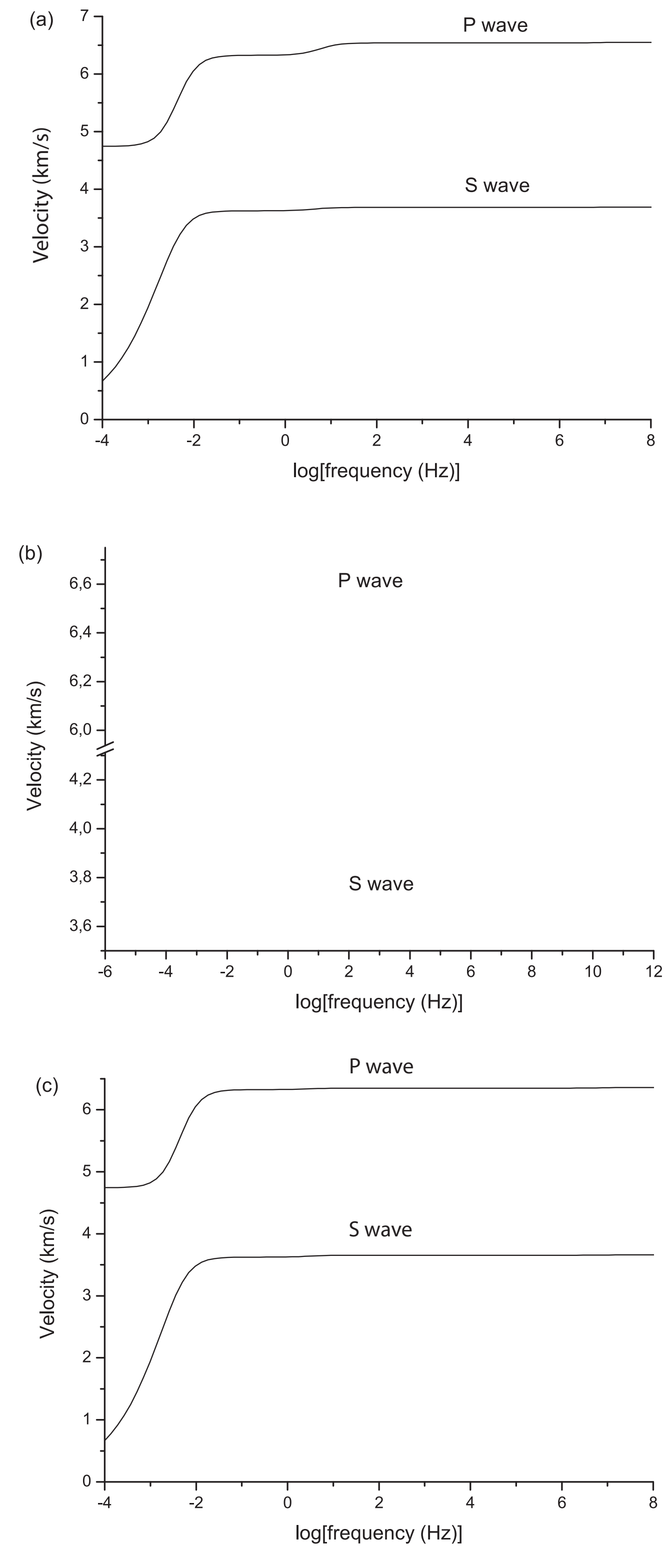

Fig. 6. Seismic velocities as a function of frequency at 6 km depth; (a) With the squirt-flow, Burgers and Biot peaks, (b) With the squirt-flow and Biot peaks, (c) With the Burgers and Biot peaks.

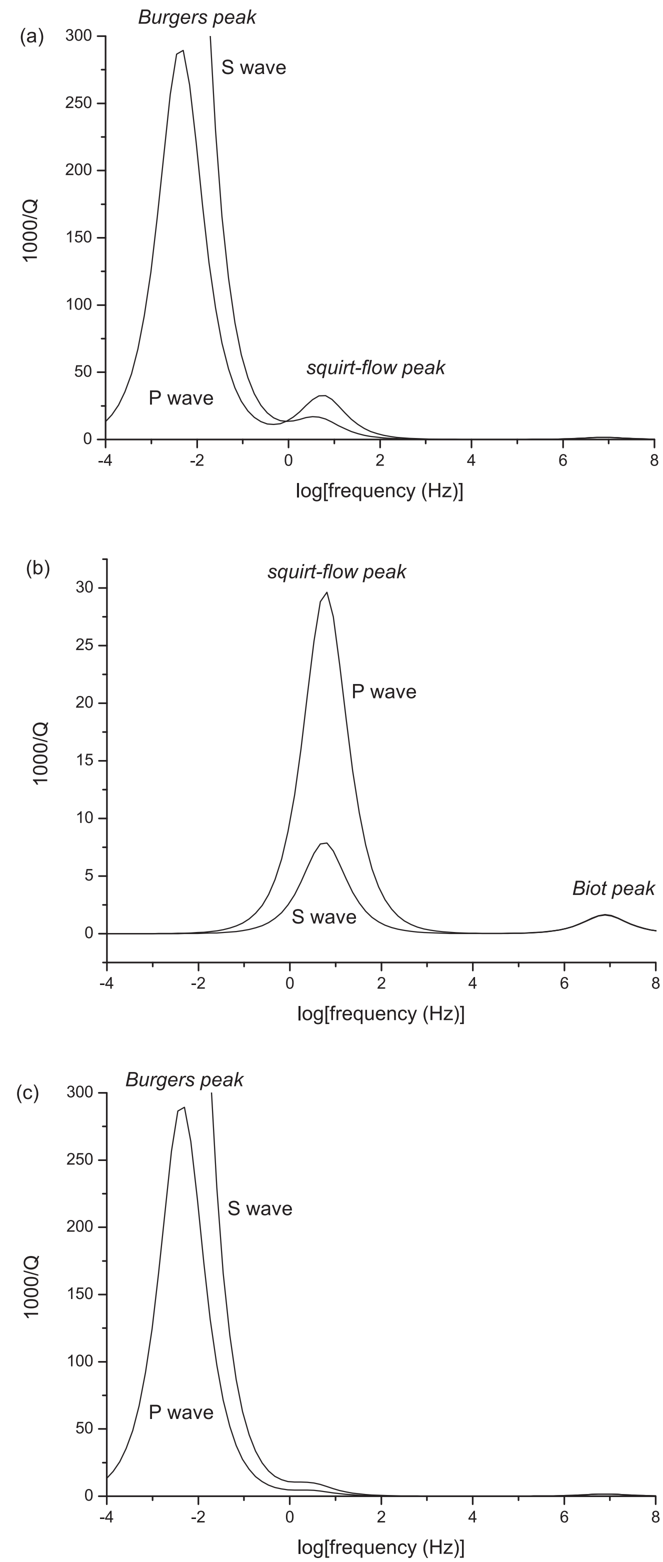

Fig. 7. Quality factors s a function of frequency at 6 km depth; (a) Squirt-flow, Burgers and Biot peaks, (b) Squirt-flow and Biot peaks, (c) Burgers and Biot peaks.

modulus can be obtained from Gassmann equation corresponding to the bulk modulus (see Eq. (7.34) in Carcione (2014)). The "crack-free" dry- and wet-rock P-wave velocities are 6670 m/s and 6770 m/s, respectively. Then, we have $K_m = K_h = \rho_s(1-\phi)[6670^2-(4/3)3880^2] = 67$ GPa and $K_G = [\phi\rho_f + (1-\phi)\rho_s][6770^2-(4/3)3820^2] = 75$ GPa. Solving the 2nd-order equation for K_s resulting from Gassmann equation, we obtain $K_s = 137$ GPa. According to Eq. (15) we have $K_0 = K_h = 67.1$ GPa and $\mu_0 = \mu_h = 41.3$ GPa. The pressure dependence is

$$g_1 = 1-(1-0.39)\exp(-p_d/50), \quad g_2 = 1-(1-0.52)\exp(-p_d/62), \tag{25}$$

where p_d is given in MPa, which is in agreement with Fig. 3 of Popp and Kern (1994). Moreover, we consider $h/R = 0.00001$ and

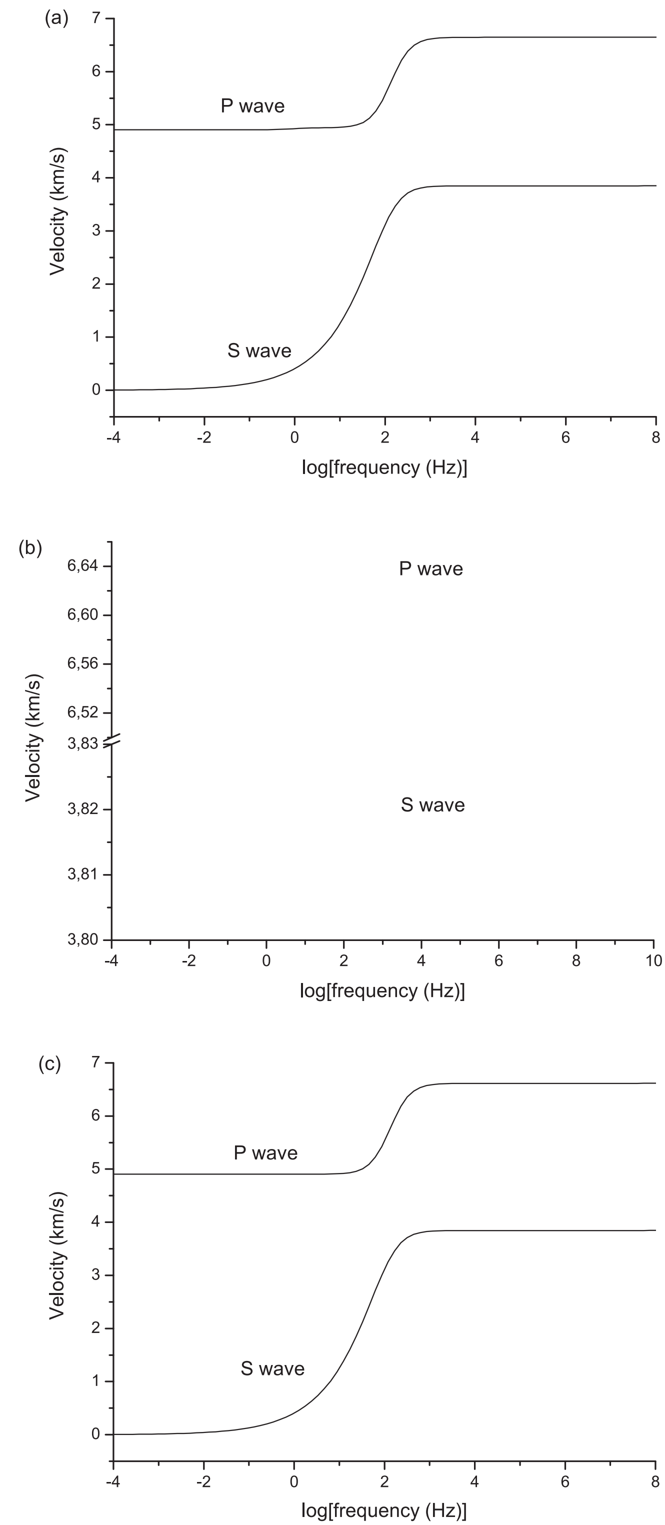

Fig. 8. Seismic velocities as a function of frequency at 12 km depth; (a) With the squirt-flow, Burgers and Biot peaks, (b) With the squirt-flow and Biot peaks, (c) With the Burgers and Biot peaks.

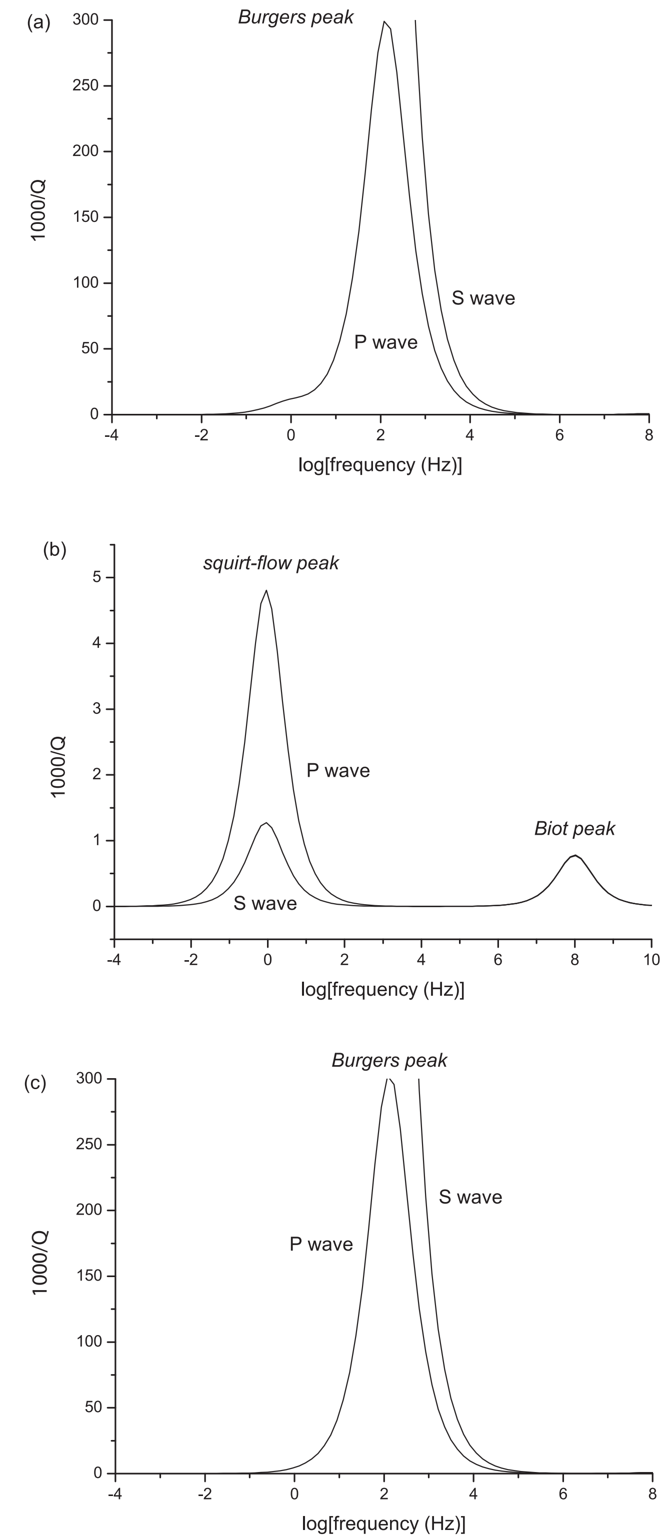

Fig. 9. Quality factors as function of frequency at 12 km depth; (a) With the squirt-flow, Burgers and Biot peaks, (b) With the squirt-flow and Biot peaks, (c) With the Burgers and Biot peaks.

$$\phi_c[\%] = 0.472\ \exp(-0.02741 p_c), \tag{26}$$

according to Fig. 5a of Popp and Kern (1994) (p_c is given in MPa). Closure of cracks with confining pressure is reflected in the values of the wet-rock crack porosity ϕ_c.

Next, we obtain the wave velocities and quality factors at different temperature-pressure conditions. The shear seismic loss parameter is obtained from empirical equations derived by Castro et al. (2008) for the crust in Southern Italy. They report $Q_0 = 18.8 f^{1.7}$ for the upper crust and up to a frequency of 10 Hz. In the examples we consider a Zener peak frequency of $f_0 = 3$ Hz, with $\omega_0 = 2\pi f_0$, which gives $Q_0 = 122$. The temperature is a function of depth through the geothermal gradient G as $T = zG$, where z is depth and $G = 60\ ^\circ$C/km in our calculations. The lithostatic stress is $\sigma_v = -\bar{\rho}gz = -p_c$, where $\bar{\rho} = 2600\,\mathrm{kg/m^3}$ is the average density and $g = 9.81\,\mathrm{m/s^2}$ is the gravity constant. To obtain the octahedral stress (4) we consider a simple model based on the gravity contribution at depth z. The horizontal stresses can be estimated as

$$\sigma_H = \frac{\nu\sigma_v}{1-\nu}, \quad \text{and } \sigma_h = \xi\sigma_H \tag{27}$$

where

$$\nu = \frac{3K_0-2\mu_0}{2(3K_0+\mu_0)} \tag{28}$$

is the Poisson ratio. The factor $\nu/(1-\nu)$ lies between 0.25 and 1 for ν ranging from 0.2 to 0.5, with the latter value corresponding to a liquid (hydrostatic stress). The parameter $\xi \leqslant 1$ has been introduced to model additional effects due to tectonic activity (anisotropic tectonic stress). Furthermore, we consider $A_\infty = 100\,(\mathrm{MPa})^{-n}\,\mathrm{s}^{-1}$, $E = 134$ kJ/mol and $n = 2.6$ (e.g., Kirby and Kronenberg, 1987), and take $\xi = 0.8$. The above degree of stress anisotropy is consistent with values at prospective depths provided by Hegret (1987) for the Canadian Shield, and in agreement with data reported in Engelder (1993, p. 91).

The water properties as a function of pressure and temperature are obtained from the fluid thermo-physical database provided in the website of the National Institute of Standards and Technology (NIST), collected from laboratory measurements by Lemmon et al. (2005). In "Thermophysical Properties of Fluid Systems", we choose water (1) and Isothermal Properties (3). The range of allowable values are [0, 1000] °C and [0, 1000] MPa. In order to analyse the seismic properties in the presence of overpressure and anomalous temperatures, we extract the water density, ρ_w, sound velocity, c_w, and viscosity from the NIST webstite for the range [0, 900] °C and [0, 200] MPa. A 3D plot is shown in Fig. 2. The part of the density surface with a value of approximately $200\,\mathrm{kg/m^3}$, delimited by 40–100 MPa and 100–200 °C, corresponds to the vapor phase. The bulk modulus is then given by $K_f = \rho_w c_w^2$.

A state of hydrostatic pore pressure is given by $p = \bar{\rho}_f gz$, where $\bar{\rho}_f = 1040\,\mathrm{kg/m^3}$ is an average fluid density. We consider a depth range [5, 15] km, where pore pressure and temperature vary from 51 to 153 MPa and 300 to 900 °C, respectively (the geothermal gradient is 60 °C/km). The experimental density, sound velocity and viscosity of water are shown in Fig. 3, together with the pressure and temperature profiles. Compare these values to the ones at ambient conditions, defined by a temperature of 20 °C and a pressure of 0.1 MPa: a water density of $998\,\mathrm{kg/m^3}$ and a sound velocity of 1482 m/s.

Next, we obtain the seismic properties using the approximation (12), which allows for numerical computations of seismograms using the Zener model (Carcione and Gurevich, 2011). Fig. 4 shows the seismic (phase) velocity (a) and quality factor (b) as a function of depth. The frequency is 10 Hz. As can be seen, the P-wave velocities decrease after a given viscosity dictated by a critical (transition) temperature (ca. 930 K) (the brittle-ductile transition) and the Arrhenius equation. The P-wave attenuation has a maximum at this transition and at higher temperatures the medium becomes a fluid whose quality factors are solely determined by the dilatational losses. Indeed, the lack of the shear losses increases the quality factor and the material behaves fluid-like with weaker attenuation. This is consistent with the fact that a pure solid and a pure liquid have weak attenuation and melting shows lower Q factors. The main contribution to anelasticity is given by the Burgers loss mechanism. Fig. 5 shows the same properties in the absence of this mechanism, where attenuation is only due to the squirt-flow mechanism, which disappears at increasing depths due to the closing of cracks. The S wave shows lower attenuation.

Figs. 6 and 7 shows the behaviour of the phase velocity and quality factor as a function of frequency for a temperature of 360 °C (the depth is 6 km), where case (a) includes the three loss mechanisms. The waves are very dispersive due to the low Q factor. The Biot peak (global flow) can be seen at high frequencies ($f_B = \phi\eta_f\rho/[2\pi\kappa\rho_f(\rho\mathcal{T}-\phi\rho_f)]$). The same properties at 12 km depth, beyond the brittle-ductile transition, are represented in Figs. 8 and 9. The Burgers peak moves towards the low frequencies at shallower depths, above the brittle-ductile transition.

The equations of motion in the space–time domain can be obtained as in Carcione and Gurevich (2011) and can be solved with numerical methods using memory variables provided the condition (11) is satisfied. Similarly, the Burgers kernel can also be implemented (Carcione et al., 2014).

5. Conclusions

The Earth crust behaves brittle and ductile depending on the in situ temperature and pressure conditions. We present a methodology to model the seismic properties of the crust, including melting, by using a poro-viscoelastic description, based on Biot theory and the Burgers and squirt-flow models. The theory describes variations of the properties due to changes in temperature and confining and pore pressure, through the dry-rock stiffness moduli. The wet-rock seismic velocities can explicitly be obtained as a function of the water properties at critical and supercritical conditions. The Burgers element allows us to model the effects of the steady-state creep flow on the dry-rock frame. The stiffness components of the brittle and ductile media depend on stress and temperature through the shear viscosity, which is obtained by the Arrhenius equation and the octahedral stress criterion. The theory generalizes a preceding theory based on Gassmann (low-frequency) moduli to the more general case of the presence of local (squirt) flow and global (Biot) flow, which contribute with additional attenuation mechanisms to the wave propagation. The squirt-flow model has a free parameter represented by the aspect ratio of the grain contacts.

Acknowledgments

We thank Aronne Craglietto for providing the NIST data.

References

Avramov, I., 2007. Viscosity activation energy. Phys. Chem. Glasses: Eur. J. Glass Sci. Technol. B 48 (1), 61–66.
Biot, M.A., 1962. Mechanics of deformation and acoustic propagation in porous media. J. Appl. Phys. 33, 1482–1498. http://dx.doi.org/10.1063/1.1728759.
Batzle, M., Han, D.-H., Hofmann, R., 2006. Fluid mobility and frequency-dependent seismic velocity – direct measurements. Geophysics 71, N1–N9.
Carcione, J.M., 2014. Wave fields in real media:wave propagation in anisotropic, anelastic, porous and electromagnetic media. In: Handbook of Geophysical Exploration. Elsevier, Amsterdam (3rd edition, revised and extended).
Carcione, J.M., Helle, H.B., Gangi, A.F., 2006. Theory of borehole stability when drilling through salt formations. Geophysics 71, F31–F47.
Carcione, J.M., Gurevich, B., 2011. Differential form and numerical implementation of Biot's poroelasticity equations with squirt dissipation. Geophysics 76, N55–N64.
Carcione, J.M., Picotti, S., 2006. P-wave seismic attenuation by slow-wave diffusion: effects of inhomogeneous rock properties. Geophysics 71, O1–O8.
Carcione, J.M., Poletto, F., 2013. Seismic rheological model and reflection coefficients of the brittle-ductile transition. Pure Appl. Geophys. 170, 2021–2035. http://dx.doi.org/10.1007/s00024-013-0643-4.
Carcione, J.M., Poletto, F., Farina, B., Craglietto, A., 2014. Simulation of seismic waves at the Earth's crust (brittle-ductile transition) based on the Burgers model. Solid Earth Discuss. 6, 1371–1400.
Carcione, J.M., Poletto, F., Farina, B., Craglietto, A., 2017. The Gassmann-Burgers model to simulate seismic waves at the Earth crust and mantle. Pure Appl. Geophys. 174, 849–863. http://dx.doi.org/10.1007/s00024-016-1437-2.
Castro, R.R., Gallipoli, M.R., Mucciarelli, M., 2008. Crustal Q in southern Italy determined from regional earthquakes. Tectonophysics 457 (2), 96–101.
Dragoni, M., Pondrelli, S., 1991. Depth of the brittle-ductile transition in a transcurrent boundary zone. Pure Appl. Geophys. 135, 447–461.
Engelder, T., 1993. Stress Regimes in the Lithosphere. Princeton University Press.
Fogler, H.S., 2005. Elements of Chemical Reaction Engineering, 4th ed. Pearson, Westford.
Gangi, A.F., 1981. A constitutive equation for one-dimensional transient and steady-state flow of solids. Mechanical Behavior of Crustal Rocks, Geophysical Monograph, 24, AGU, 275–285.
Gangi, A.F., 1983. Transient and steady-state deformation of synthetic rocksalt. Tectonophysics 91, 137–156.

Gurevich, B., Makarynska, D., Pervukhina, M., De Paula, O., 2010. A simple model for squirt-flow dispersion and attenuation in fluid-saturated granular rocks. Geophysics 75 (6), N109–N120. http://dx.doi.org/10.1190/1.3509782.
Hegret, G., 1987. Stress assumption for underground excavation in the Canadian Shield. Int. J. Rock Mech. Min. Sci. Geomech. Abstr. 24, 95–97.
Hoshiba, M., 1993. Separation of scattering attenuation and intrinsic absorption in Japan using the multiple lapse time window analysis of full seismogram envelope. J. Geophys. Res. 98, 15809–15824.
Karato, S., 2014. Does partial melting explain geophysical anomalies? Phys. Earth Planet. Int. 228, 300–306.
Karato, S., Jung, H., 1998. Water, partial melting and the origin of seismic low velocity and high attenuation zone in the upper mantle. Earth Planet. Sci. Lett. 157, 193–207.
Kaselow, A., Shapiro, S.A., 2004. Stress sensitivity of elastic moduli and electrical resistivity in porous rocks. J. Geophys. Eng. 1, 1–11.
Kirby, S.H., Kronenberg, A.K., 1987. Rheology of the lithosphere; selected topics. Rev. Geophys. 25, 1219–1244.
Lemmon, E.W., McLinden, M.O., Friend, D.G., 2005. Thermophysical properties of fluid systems. In: Lindstrom, P.J., Mallard, W.G. (Eds.), NIST Chemistry Webbook 69, NIST Standard Reference Database, Gaithersburg, MD, USA. < http://webbook.nist.gov/chemistry/ > .
Manning, C.E., Ingebritsen, S.E., 1999. Permeability of the continental crust: the implications of geothermal data and metamorphic systems. Rev. Geophys. 37, 127–150.
Mavko, G., Jizba, D., 1991. Estimating grain-scale fluid effects on velocity dispersion in rocks. Geophysics 56, 1940–1949.
Mavko, G., Mukerji, T., Dvorkin, J., 2009. The Rock Physics Handbook: Tools for Seismic Analysis in Porous Media. Cambridge Univ. Press.
Mavko, G., Nur, A., 1975. Melt squirt in the asthenosphere. J. Geophys. Res. 80, 1444–1448.
Meissner, R., Strehlau, J., 1982. Limits of stresses in continental crusts and their relation to the depth-frequency distribution of shallow earthquakes. Tectonics 1, 73–89.
Montesi, L.G.J., 2007. A constitutive model for layer development in shear zones near the brittle-ductile transition. Geophys. Res. Lett. 34, L08307. http://dx.doi.org/10.1029/2007GL029250.
Popp, T., Kern, H., 1994. The influence of dry and water saturated cracks on seismic velocities of crustal rocks – a comparison of experimental data with theoretical model. Surv. Geophys. 15, 443–465.
Pride, S.R., Berryman, J.G., Harris, J.M., 2004. Seismic attenuation due to wave-induced flow. J. Geophys. Res. 109, B01201. http://dx.doi.org/10.1029/2003JB002639.
Rachman, A.N., Chung, T.W., 2016. Depth-dependent crustal scattering attenuation revealed using single or few events in South Korea. Bull. Seismol. Soc. Am. 106 (4), 1499–1508.
Ranalli, G., 1997. Rheology of the lithosphere in space and time Geological Society, London. Spec. Publ. 121, 19–37.
Schmeling, H., 1985. Numerical models on the influence of partial melt on elastic, anelastic and electric properties of rocks. Part I. Elasticity and anelasticity. Phys. Earth Planet. Int. 41, 34–57.
Takei, Y., 2002. Effect of pore geometry on V_P/V_S: from equilibrium geometry to crack. J. Geophys. Res. 107. http://dx.doi.org/10.1029/2001JB000522.
Tauzin, B., Debayle, E., Wittinger, G., 2010. Seismic evidence for a global low velocity layer within the Earth's upper mantle. Nat. Geosci. 3, 718–721.
Walsh, J.B., 1969. A new analysis off attenuation in partially melted rock. J. Geophys. Res. 74, 4333–4337.
Williams, Q., Garnero, E.J., 1996. Seismic evidence for partial melt at the base of Earth's mantle. Science 273, 1528–1530.